

Quasi-one- and quasi-two-dimensional Bose-Fermi mixtures from weak coupling to unitarity

Pardeep Kaur* · Sandeep Gautam** ·
S. K. Adhikari***

Received: date / Accepted: date

Abstract We study ultracold superfluid Bose-Fermi mixtures in three dimensions, with stronger confinement along one or two directions, using a non-perturbative beyond-mean-field model for bulk chemical potential valid along the weak-coupling to unitarity crossover. Although bosons are considered to be in a superfluid state, we consider two possibilities for the fermions – spin-polarized degenerate state and superfluid state. Simplified reduced analytic lower-dimensional models are derived along the weak-coupling to unitarity crossover in quasi-one-dimensional (quasi-1D) and quasi-two-dimensional (quasi-2D) settings. The only parameters in these models are the constants of the beyond-mean-field Bose-Bose and Fermi-Fermi Lee-Huang-Yang interactions and the respective universal Bertsch parameter at unitarity. In addition to the numerical results for a fully-trapped system, we also present results for quasi-2D Bose-Fermi mixtures where one of the components is untrapped but localized due to the interaction mediated by the other component. We demonstrate the validity of the reduced quasi-1D and quasi-2D models via a comparison of the numerical solutions for the ground states obtained from the reduced models and the full three-dimensional (3D) model.

1 Introduction

For the last two decades or so, both experimental [1–4] and theoretical [5–7] investigations have been undertaken on the two-component mixtures of quantum degenerate atomic gases. While the initial studies mainly focused on the degenerate Bose-Bose mixtures, later with the experimental realization of stable quantum degenerate Bose-Fermi mixtures consisting of a superfluid Bose gas and a spin-polarized degenerate Fermi gas [8–19], these systems

* 2018phz0004@iitrpr.ac.in

** sandeep@iitrpr.ac.in

*** sk.adhikari@unesp.br

*Department of Physics, Indian Institute of Technology Ropar, Rupnagar, Punjab 140001, India, ·
Department of Physics, Indian Institute of Technology Ropar, Rupnagar, Punjab 140001, India, *Instituto de Física Teórica, UNESP - Universidade Estadual Paulista, 01.140-070 São Paulo, São Paulo, Brazil.

attracted particular interest. The quantum degenerate Bose-Fermi mixtures of ^{87}Rb - ^{40}K [8–12], ^{23}Na - ^6Li [13], ^7Li - ^6Li [14], ^{87}Rb - ^{171}Yb [15], ^{41}K - ^6Li [16], ^{174}Yb - ^6Li [17], ^{133}Cs - ^6Li [18, 19], etc. are among the experimental realizations of such systems. These Bose-Fermi quantum degenerate mixtures have mass imbalance ranging from a small to a large value. With a lighter fermionic component (^6Li) and a heavier bosonic component (^{133}Cs), ^{133}Cs - ^6Li quantum degenerate mixture has a large mass imbalance that offers rich interaction properties that are well characterized [20–24]. In a recent experiment Desalvo *et al.* [19] showed that in a Bose-Einstein condensate (BEC) of caesium atoms inside a spin-polarized quantum degenerate Fermi gas of lithium atoms, interspecies interactions can lead to an effective trapping potential via a fermion-mediated attractive boson-boson interactions. Earlier in another experiment, Desalvo *et al.* [18] had showed that a spin-polarized degenerate Fermi gas of ^6Li , even without an external trapping, can be fully confined in a harmonically trapped ^{133}Cs BEC. These degenerate Bose-Fermi mixtures also paved the way to realize self-trapped entities termed as soliton trains [19, 25, 26].

To study a superfluid Bose-Fermi mixture, the mean-field treatment is commonly used, which accounts for the weakly-interacting limit of interactions in the mixture, encapsulated by the Gross-Pitaevskii (GP) equation for bosons [27–29] and Bardeen-Cooper-Schrieffer (BCS) mean-field equations for fermions [30]. In the case of fermions, simpler superfluid hydrodynamic equations are commonly used to study the physics characterized by wavelengths longer than the healing length [31, 32]. These superfluid hydrodynamic equations are equivalent to a time-dependent non-linear Schrödinger equation which can be used to study the macroscopic properties of these weakly-interacting superfluids including collective excitations [33–37]. To account for strong interactions, crossover models have also been proposed in the literature that connect weak-coupling and unitarity limits for bosons [38, 39] and fermions [39–41]. The crossover model for fermions enjoyed widespread usage [42–46]. Nonetheless, interspecies Bose-Fermi interaction in these studies still corresponds to weakly-interacting domain. Lee, Huang, and Yang [47] (LHY) provided the lowest-order beyond-mean-field correction to energy for the Bose [48] and Fermi [49] systems, which played a vital role in the development of these crossover models. Usually, these crossover models [38–40] for Bose and Fermi systems produce the correct weak-coupling LHY as well as the strong-coupling unitarity limits. However, these crossover models for Bose and Fermi interactions, for describing the superfluid Bose-Fermi mixtures between weak- and strong-coupling regimes, usually have fitting parameters. In this study, we propose minimal crossover models without adjustable fitting parameters to describe the Bose and Fermi interactions from the weak-coupling to unitarity limits for quasi-one-dimensional (quasi-1D) and quasi-two-dimensional (quasi-2D) configurations. These are derived from the corresponding three-dimensional (3D) model, by integrating out the dependence on the transverse coordinates by the usual procedure [50]. The only parameters in these reduced quasi-1D and quasi-2D models are the constants of the Bose-Bose and Fermi-Fermi LHY interactions and the universal Bertsch parameter [51] at unitarity. We also present the relevant equations for a degenerate Bose-Fermi mixture in 3D, quasi-1D and quasi-2D configurations, as many of the experiments were performed under these conditions. In this case the energy of the bosons is described by the crossover model varying from weak-coupling to unitarity limit, whereas that of the noninteracting degenerate fermions has the contribution from the Fermi pressure term only.

Using the analytic weak-coupling to unitary crossover functions for bulk chemical potentials and energy densities of Bose and Fermi components, we write the 3D beyond mean-field equations for both a superfluid and a degenerate Bose-Fermi mixture valid along the crossover from the weak-coupling to the unitarity limits, from which the reduced quasi-1D

and quasi-2D model equations are derived. The quasi-1D and quasi-2D traps are of interest as many experiments are performed in these settings. The resulting coupled non-linear Schrödinger equation has bulk chemical potentials in the form of analytic Padé approximants connecting the weak and strong coupling limits. We use these crossover models to study Bose-Fermi mixtures confined by quasi-1D and quasi-2D trapping potentials, and compare the results of atom densities with those obtained from the 3D crossover model. The Bose-Fermi mixture is miscible (immiscible) for weak (strong) Bose-Fermi repulsion [52–57]. Here we consider miscible as well as phase-separated Bose-Fermi mixtures for repulsive Bose-Bose and Bose-Fermi interactions. In addition to the study of fully-trapped systems with repulsive Bose-Bose and Bose-Fermi interactions, we also consider the problem of self-trapping of one of the components as a result of the interactions mediated by the other component in quasi-2D Bose-Fermi superfluid and degenerate mixtures for attractive Bose-Fermi and repulsive Bose-Bose interactions, as explored in recent experiments [18, 19] for a degenerate Bose-Fermi mixture.

The following depicts how the paper is arranged. The analytical equations for the energy density and bulk chemical potential of homogeneous Bose and Fermi superfluids along with those of spin-polarized degenerate Fermi gas in three dimensions along the weak coupling to unitarity crossover are presented in Sec. 2. In Sec. 3, we derive the analytic expressions for energy density and bulk chemical potential for bosons in quasi-1D and quasi-2D configurations along the weak coupling to unitarity crossover and derive the respective nonlinear Schrödinger equations. In Sec. 4, we derive the same for fermions in quasi-1D and quasi-2D configurations. In Sec. 5, we derive the crossover model for superfluid and degenerate Bose-Fermi mixtures in quasi-1D, quasi-2D and 3D configurations in dimensionless units valid along the weak-coupling to unitarity limits for intraspecies interactions. The interspecies interaction is taken to be in the weakly interacting regime. In Sec. 6, we first present numerical results for phase-separated and miscible quasi-1D and quasi-2D Bose-Fermi superfluid mixtures and later numerical results for Bose (Fermi) mediated trapping of Fermi (Bose) superfluid component in quasi-2D mixtures using the full 3D and reduced models. We also present results for Bose (Fermi) mediated trapping of Fermi (Bose) component in quasi-2D degenerate Bose-Fermi mixtures using the full 3D and reduced models. In Sec. 7 we present a brief summary of this study.

2 Super-fluid hydrodynamics and nonlinear equations

In the unitarity limit, $|a_i| \rightarrow \infty$ resulting in a Bose/Fermi superfluid system of N_i atoms with a universal behavior [58–63] governed by particle density n_i alone, where a_i is the intraspecies scattering length. Here $i = B$ for bosons and $i = F$ for paired fermions. The bulk chemical potential of a homogeneous Bose or Fermi gas at unitarity is [30, 39]

$$\lim_{|a_i| \rightarrow \infty} \mu_i(n_i, a_i) = \frac{\hbar^2}{m_i} \eta_i n_i^{2/3}, \quad (1)$$

where η_i is the universal Bertsch parameter [51], and m_i is the mass of an atom. By dimensional argument Eq. (1) is the simplest expression with the dimension of energy using particle density n_i .

The bulk chemical potential μ_B of a homogeneous Bose gas in the weak-coupling limit is given by [48]

$$\mu_B(n_B, a_B) = \frac{\hbar^2}{m_B} (4\pi n_B a_B + 2\pi\alpha n_B^{3/2} a_B^{5/2} + \dots), \quad (2)$$

where $\alpha = 64/(3\sqrt{\pi})$. The first term in this expression for μ_B is the mean-field GP chemical potential per particle [28, 29] and the second term is the perturbative LHY correction [48] to it; the latter is meaningful only for small to moderate values of the scattering length a_B (> 0). The *minimal* or the simplest analytic form of the non-perturbative bulk chemical potential along the crossover between weak coupling to unitarity is [41]

$$\mu_B(n_B, a_B) \equiv \frac{\hbar^2}{m_B} n_B^{2/3} f(\tau), \quad \tau = a_B n_B^{1/3}, \quad (3)$$

$$f(\tau) = 4\pi \frac{\tau + \alpha \tau^{5/2}}{1 + \frac{\alpha}{2} \tau^{3/2} + \frac{4\pi\alpha}{\eta_B} \tau^{5/2}}, \quad (4)$$

which has the correct unitarity and weak-coupling limits, viz. Eqs. (1) and (2), respectively. Expression (4) is written in a numerator-over-denominator form like a Padé-type approximant and is valid for all values of the scattering length a_B joining the weak-coupling and unitarity limits. The bulk chemical potential μ_i and energy density \mathcal{E}_i of a homogeneous Bose or Fermi system are related by

$$\mu_i(n_i, a_i) = \frac{\partial [n_i \mathcal{E}_i(n_i, a_i)]}{\partial n_i}, \quad (5)$$

or, equivalently, by

$$\mathcal{E}_i(n_i, a_i) = \frac{1}{n_i} \int_0^{n_i} \mu_i(n, a_i) dn. \quad (6)$$

Using Eq. (6), the bosonic energy density consistent with Eq. (2), valid in the weak-coupling limit, is

$$\begin{aligned} \mathcal{E}_B(n_B, a_B) &\equiv \frac{1}{n_B} \int_0^{n_B} \mu_B(n, a_B) dn \\ &= \frac{\hbar^2}{m_B} \left(2\pi n_B a_B + \frac{4}{5} \pi \alpha n_B^{3/2} a_B^{5/2} + \dots \right), \end{aligned} \quad (7)$$

and the same at unitarity, in accordance with Eq. (1), is

$$\mathcal{E}_B(n_B, a_B) = \frac{\hbar^2}{m_B} \frac{3}{5} \eta_B n_B^{2/3}. \quad (8)$$

The following Padé-type approximant for the energy density valid along the weak-coupling to unitarity crossover [41]

$$\mathcal{E}_B(n_B, a_B) \equiv \frac{\hbar^2}{m_B} \frac{2\pi n_B^{2/3} (\tau + \frac{4\alpha}{5} \tau^{5/2})}{1 + \frac{2\alpha}{5} \tau^{3/2} + \frac{8\pi\alpha}{3\eta_B} \tau^{5/2}}, \quad (9)$$

reduces to Eqs. (7) and (8) in weak-coupling and unitarity limits, respectively.

In the weak-coupling limit, the energy density of a homogeneous superfluid of spin-1/2 Fermi gas with an equal population of spin-up and -down fermions is given by [30, 49]

$$\mathcal{E}_F(n_F, a_F) = \frac{3}{5} E_F [1 + c_1 \kappa + c_2 \kappa^2 + \dots], \quad (10)$$

$$c_1 = \frac{10}{9\pi}, \quad c_2 = \frac{4(11 - \ln 4)}{21\pi^2}, \quad \kappa = k_F a_F, \quad (11)$$

with Fermi momentum $k_F = (3\pi^2 n_F)^{1/3}$, Fermi energy $E_F = \hbar^2 k_F^2 / 2m_F$, and $a_F (< 0)$ the s -wave scattering length corresponding to the scattering between spin up-down fermions. In Eq. (10), the first term $3E_F/5$ is the density-functional term [30, 39] valid in the BCS [64] weak-coupling limit ($a_F \rightarrow 0^-$) and the following two terms are the perturbative LHY corrections [49] valid for small to medium values of $|a_F|$. The unitarity limit of energy density is written as [39]

$$\lim_{|a_F| \rightarrow \infty} \mathcal{E}_F(n_F, a_F) = \frac{3}{5} E_F \eta_F. \quad (12)$$

The following minimal analytic energy density along the crossover between weak-coupling to unitarity regimes [41]

$$\mathcal{E}_F(n_F, a_F) = \frac{3}{5} E_F \left[1 + \frac{c_1 \kappa + (c_2 - 2c_1^2) \kappa^2}{1 - 2c_1 \kappa + \frac{(c_2 - 2c_1^2) \kappa^2}{\eta_F - 1}} \right], \quad (13)$$

reduces to Eqs. (10) and (12) in the weak-coupling and unitarity limits, respectively. Again, expression (13) is a Padé-type approximant derived from Eqs. (10) and (12).

From Eqs. (5) and (10), the bulk chemical potential of a homogeneous superfluid Fermi gas in the weak-coupling limit is

$$\mu_F(n_F, a_F) \equiv \frac{\partial(n_F \mathcal{E}_F)}{\partial n_F} = E_F [1 + d_1 \kappa + d_2 \kappa^2 + \dots], \quad (14)$$

$$d_1 = \frac{4}{3\pi}, \quad d_2 = \frac{4(11 - \ln 4)}{15\pi^2}, \quad (15)$$

and similarly in the unitarity limit from Eqs. (5) and (12), we get for the bulk chemical potential

$$\lim_{|a_F| \rightarrow \infty} \mu_F(n_F, a_F) = E_F \eta_F. \quad (16)$$

The non-perturbative bulk chemical potential along the weak-coupling to unitarity crossover is the following Padé-type approximant derived from Eqs. (14) and (16) [41]

$$\mu_F(n_F, a_F) \equiv E_F g(\kappa), \quad (17)$$

$$g(\kappa) = \left[1 + \frac{d_1 \kappa + (d_2 - 2d_1^2) \kappa^2}{1 - 2d_1 \kappa + \frac{(d_2 - 2d_1^2) \kappa^2}{\eta_F - 1}} \right]. \quad (18)$$

For a noninteracting spin-polarized degenerate Fermi gas the energy density is given by the so called Fermi pressure term

$$\mathcal{E}_F(n_F) = \frac{3}{5} E_F \quad (19)$$

but now with Fermi momentum $k_F = (6\pi^2 n_F)^{1/3}$ and Fermi energy $E_F = \hbar^2 k_F^2 / 2m_F$. The difference of a factor of 2 in the Fermi momentum is due to the fact that each energy level can now accommodate only one spin-polarized fermion and not two as in the case of the superfluid composed of an equal-number mixture of spin-up and -down fermions. In the case of a *noninteracting* spin-polarized degenerate Fermi gas the bulk chemical potential is

$$\mu_F(n_F) = E_F \quad (20)$$

and both the energy density and the bulk chemical potential are independent of scattering length. Interaction or scattering, via s -partial wave, between two spin-polarized fermions is forbidden by the Pauli exclusion principle.

We consider a Bose/Fermi superfluid in a highly anisotropic harmonic trapping potential,

$$V_i(x, y, z) = \frac{1}{2} m_i \omega_i^2 (\lambda^2 x^2 + \nu^2 y^2 + \gamma^2 z^2), \quad (21)$$

where $\lambda \equiv \omega_x/\omega_i$, $\nu \equiv \omega_y/\omega_i$, and $\gamma \equiv \omega_z/\omega_i$ are trap-anisotropy parameters along x , y and z directions, respectively, and where ω_x , ω_y and ω_z are angular frequencies of the harmonic traps, respectively, along x , y and z axes, and ω_i is a reference frequency that will be defined later. The trap-anisotropy parameters – λ , ν and γ – are taken to be the same for bosons and fermions, although this restriction can be easily removed.

In the quasi-1D configuration, $\lambda \ll \nu, \gamma$; the 3D wave-function can be approximated as [50]

$$\phi_i^{3D}(\mathbf{r}, t) = \phi_i^{1D}(x, t) \Phi_i^{2D}(y, z), \quad (22)$$

where the dynamics described by the 1D wave function $\phi_i^{1D}(x, t)$ is confined along the x direction and in the transverse (y, z) directions the dynamics is considered frozen in the stationary harmonic-oscillator ground state

$$\Phi_i^{2D}(y, z) = (\pi d_z^2)^{-1/4} (\pi d_y^2)^{-1/4} e^{-z^2/2d_z^2} e^{-y^2/2d_y^2}, \quad (23)$$

of the trapping potential $m_i \omega_i^2 (\nu^2 y^2 + \gamma^2 z^2)/2$, where $d_z = l_i/\sqrt{\gamma}$ and $d_y = l_i/\sqrt{\nu}$ with $l_i = \sqrt{\hbar/(m_i \omega_i)}$. In this case it is convenient to take $\omega_i = \omega_x$. The bulk chemical potential and bosonic energy density, obtained by conveniently integrating out the y and z dependence, will now have the following 1D forms [50]

$$\mu_i^{1D}(n_i^{1D}, a_i) = \int \mu_i(n_i, a_i) |\Phi_i^{2D}(y, z)|^2 dy dz, \quad (24)$$

$$\mathcal{E}_i^{1D}(n_i^{1D}, a_i) = \int \mathcal{E}_i(n_i, a_i) |\Phi_i^{2D}(y, z)|^2 dy dz, \quad (25)$$

where the 1D density is given by $n_i^{1D} = N_i |\phi_i^{1D}(x, t)|^2$.

In the quasi-2D case, $\gamma \gg \lambda, \nu$; the 3D wave-function can be approximated as

$$\phi_i^{3D}(\mathbf{r}, t) = \phi_i^{2D}(x, y, t) \Phi_i^{1D}(z), \quad (26)$$

where the dynamics described by the wave function $\phi_i^{2D}(x, y, t)$ is confined in the x - y plane and the transverse dynamics along z direction is considered frozen in the stationary harmonic-oscillator ground state

$$\Phi_i^{1D}(z) = (\pi d_z^2)^{-1/4} \exp(-z^2/2d_z^2), \quad d_z = l_i/\sqrt{\gamma}, \quad (27)$$

of the trapping potential $m_i \omega_i^2 \gamma^2 z^2/2$ with $l_i = \sqrt{\hbar/m_i \omega_i}$. Here it is convenient to take $\omega_i = \sqrt{\omega_x \omega_y}$. The bulk chemical potential and energy density will now have the following 2D forms [50]

$$\mu_i^{2D}(n_i^{2D}, a_i) = \int \mu_i(n_i, a_i) |\Phi_i^{1D}(z)|^2 dz, \quad (28)$$

$$\mathcal{E}_i^{2D}(n_i^{2D}, a_i) = \int \mathcal{E}_i(n_i, a_i) |\Phi_i^{1D}(z)|^2 dz, \quad (29)$$

where the 2D density is now given by $n_i^{2D} = N_i |\phi_i^{2D}(x, y, t)|^2$.

The dynamical equation for a Bose/Fermi superfluid in the anisotropic trap (21) is given by

$$i\hbar \frac{\partial \phi_i^{3D}(x, y, z, t)}{\partial t} = \left[-\frac{\hbar^2}{2\beta m_i} \left\{ \frac{\partial^2}{\partial x^2} + \frac{\partial^2}{\partial y^2} + \frac{\partial^2}{\partial z^2} \right\} + V_i(x, y, z) + \mu_i(n_i, a_i) \right] \phi_i^{3D}(x, y, z, t), \quad (30)$$

where $\beta = 1$ for superfluid bosons and $\beta = 4$ for superfluid fermions [39, 41] as well as for degenerate fermions [65, 66]. Actually, for superfluid fermions the dynamical equation can be written only for a pair of fermions of mass $2m_F$, and the anomalous factor β appears after transforming the same for a single fermion of mass m_F . A similar factor has also been used in the case of degenerate fermions because of phenomenological reasons [65–69].

3 Quasi-1D and Quasi-2D reduction for bosons

3.1 Quasi-1D configuration

For bosons, in the quasi-1D case, with tight binding in the transverse y and z directions ($\lambda \ll \nu, \gamma$), using Eqs. (1) and (8) in Eqs. (24) and (25), respectively, at unitarity, we obtain the following expressions for the bulk chemical potential and energy density

$$\lim_{a_B \rightarrow \infty} \mu_B^{1D}(n_B^{1D}, a_B) = \frac{\hbar^2}{m_B} \frac{3\eta_B}{5\pi^{2/3}} \delta^{2/3}, \quad \delta = \frac{n_B^{1D}}{d_y d_z}, \quad (31)$$

$$\lim_{a_B \rightarrow \infty} \mathcal{E}_B^{1D}(n_B^{1D}, a_B) = \frac{\hbar^2}{m_B} \frac{9\eta_B}{25\pi^{2/3}} \delta^{2/3}. \quad (32)$$

Similarly, in the weakly interacting domain ($a_B \rightarrow 0$), Eqs. (2) and (7) for the 3D bulk chemical potential and energy density with LHY correction, when inserted into Eqs. (24) and (25), respectively, yield the following quasi-1D forms for the same

$$\mu_B^{1D}(n_B^{1D}, a_B) = \frac{2\hbar^2}{m_B} \delta \left[a_B + \frac{2\alpha}{5\sqrt{\pi}} a_B^{5/2} \delta^{1/2} \right], \quad (33)$$

$$\mathcal{E}_B^{1D}(n_B^{1D}, a_B) = \frac{\hbar^2}{m_B} \delta \left[a_B + \frac{8\alpha}{25\sqrt{\pi}} a_B^{5/2} \delta^{1/2} \right]. \quad (34)$$

Equations (31)–(32) and (33)–(34) lead to the following Padé-type approximants for the quasi-1D chemical potential and energy density along the crossover between weak-coupling and unitarity limits:

$$\mu_B^{1D}(n_B^{1D}, a_B) = \frac{\frac{2\hbar^2}{m_B} \delta \left[a_B + \frac{4\alpha}{5\sqrt{\pi}} a_B^{5/2} \delta^{1/2} \right]}{1 + \frac{2\alpha}{5\sqrt{\pi}} a_B^{3/2} \delta^{1/2} + \frac{8\alpha\pi^{1/6}}{3\eta_B} a_B^{5/2} \delta^{5/6}}, \quad (35)$$

$$\mathcal{E}_B^{1D}(n_B^{1D}, a_B) = \frac{\frac{\hbar^2}{m_B} \delta \left[a_B + \frac{16\alpha}{25\sqrt{\pi}} a_B^{5/2} \delta^{1/2} \right]}{1 + \frac{8\alpha}{25\sqrt{\pi}} a_B^{3/2} \delta^{1/2} + \frac{16\alpha\pi^{1/6}}{9\eta_B} a_B^{5/2} \delta^{5/6}}. \quad (36)$$

If we substitute the wave function defined by Eqs. (22) and (23) in the dynamical equation (30) and integrate the linear part of this equation over the transverse variables y and

z , following Ref. [50], and use the reduced quasi-1D model bulk chemical potential (35) in the resultant equation, we obtain the following quasi-1D nonlinear Schrödinger equation for relevant dynamics in the x direction for the Bose superfluid along the crossover, valid between weak coupling and unitarity limits

$$i\hbar \frac{\partial \phi_B^{1D}(x,t)}{\partial t} = \left[-\frac{\hbar^2}{2m_B} \frac{\partial^2}{\partial x^2} + \frac{1}{2} m_B \omega_B^2 \lambda^2 x^2 + \mu_B^{1D}(n_B^{1D}, a_B) \right] \phi_B^{1D}(x,t), \quad (37)$$

with the normalization $\int dx |\phi_B^{1D}(x,t)|^2 = 1$, where $i = \sqrt{-1}$. To handle this equation efficiently in a dimensionless form, we express length in units of $l_B \equiv \sqrt{\hbar/m_B \omega_B}$, time in units of $m_B l_B^2 / \hbar = \omega_B^{-1}$, density $n_B^{1D} \equiv |\phi_B^{1D}|^2$ in units of l_B^{-1} , and energy in units of $\hbar^2/m_B l_B^2 = \hbar \omega_B$, etc. Consequently, we obtain the following dimensionless equation for the relevant dynamics of the quasi-1D Bose superfluid along the x direction

$$i \frac{\partial \tilde{\phi}_B^{1D}(\tilde{x}, \tilde{t})}{\partial \tilde{t}} = \left[-\frac{1}{2} \frac{\partial^2}{\partial \tilde{x}^2} + \frac{1}{2} \lambda^2 \tilde{x}^2 + \tilde{\mu}_B^{1D}(\tilde{n}_B^{1D}, \tilde{a}_B) \right] \tilde{\phi}_B^{1D}(\tilde{x}, \tilde{t}), \quad (38)$$

where the quantities with tildes are dimensionless. The transverse dynamics along y, z directions are considered to be frozen in the respective harmonic-oscillator ground state. Using Eq. (35), we obtain the following dimensionless bulk chemical potential to be used in the reduced quasi-1D dynamical equation (38)

$$\tilde{\mu}_B^{1D}(\tilde{n}_B^{1D}, \tilde{a}_B) = \frac{2\tilde{\delta} \left[\tilde{a}_B + \frac{4\alpha\sqrt{\tilde{\delta}}}{5\sqrt{\pi}} \tilde{a}_B^{5/2} \right]}{1 + \frac{2\alpha}{5\sqrt{\pi}} \tilde{a}_B^{3/2} \tilde{\delta}^{1/2} + \frac{8\alpha\pi^{1/6}}{3\eta_B} \tilde{a}_B^{5/2} \tilde{\delta}^{5/6}}, \quad (39)$$

where $\tilde{\delta} = \sqrt{\nu \tilde{\gamma} \tilde{n}_B^{1D}}$.

3.2 Quasi-2D configuration

In the quasi-2D case, with tight binding in the transverse z direction ($\lambda, \nu \ll \gamma$), using Eqs. (1) and (8) for bosons in Eqs. (28) and (29), respectively, at unitarity, we obtain the following expressions for bulk chemical potential and energy density

$$\lim_{a_B \rightarrow \infty} \mu_B^{2D}(n_B^{2D}, a_B) = \frac{\hbar^2}{m_B} \frac{\sqrt{3}\eta_B}{\sqrt{5}\pi^{1/3}} \varepsilon^{2/3}, \quad \varepsilon = \frac{n_B^{2D}}{d_z}, \quad (40)$$

$$\lim_{a_B \rightarrow \infty} \mathcal{E}_B^{2D}(n_B^{2D}, a_B) = \frac{\hbar^2}{m_B} \frac{3\sqrt{3}\eta_B}{5\sqrt{5}\pi^{1/3}} \varepsilon^{2/3}. \quad (41)$$

In the weakly interacting domain ($a_B \rightarrow 0$), Eqs. (2) and (7) for the 3D bulk chemical potential and energy density with LHY correction, when substituted into Eqs. (28) and (29), respectively, yield the following quasi-2D forms for the same quantities

$$\mu_B^{2D}(n_B^{2D}, a_B) = \frac{\hbar^2}{m_B} 2\sqrt{2\pi}\varepsilon \left[a_B + \frac{\alpha\sqrt{\varepsilon} a_B^{5/2}}{\sqrt{5\sqrt{\pi}}} \right], \quad (42)$$

$$\mathcal{E}_B^{2D}(n_B^{2D}, a_B) = \frac{\hbar^2}{m_B} \sqrt{2\pi}\varepsilon \left[a_B + \frac{4\alpha\sqrt{\varepsilon} a_B^{5/2}}{5\sqrt{5\sqrt{\pi}}} \right]. \quad (43)$$

Equations (40) and (42), and (41) and (43), respectively, yield the following Padé-type approximants for the quasi-2D chemical potential and energy density valid along the weak coupling to unitarity crossover:

$$\mu_B^{2D}(n_B^{2D}, a_B) = \frac{\frac{\hbar^2}{m_B} 2\sqrt{2\pi}\varepsilon \left[a_B + \frac{2\alpha\sqrt{\varepsilon}a_B^{5/2}}{\sqrt{5\sqrt{\pi}}} \right]}{1 + \frac{\alpha\sqrt{\varepsilon}a_B^{3/2}}{\sqrt{5\sqrt{\pi}}} + \frac{4\sqrt{2\pi}\alpha\pi^{1/12}\varepsilon^{5/6}a_B^{5/2}}{\sqrt{3}\eta_B}}, \quad (44)$$

$$\mathcal{E}_B^{2D}(n_B^{2D}, a_B) = \frac{\frac{\hbar^2}{m_B} \sqrt{2\pi}\varepsilon \left[a_B + \frac{8\alpha\sqrt{\varepsilon}a_B^{5/2}}{5\sqrt{5\sqrt{\pi}}} \right]}{1 + \frac{4\alpha\sqrt{\varepsilon}a_B^{3/2}}{5\sqrt{5\sqrt{\pi}}} + \frac{8\sqrt{2\pi}\alpha\pi^{1/12}\varepsilon^{5/6}a_B^{5/2}}{3\sqrt{3}\eta_B}}. \quad (45)$$

If we substitute the wave function defined by Eqs. (26) and (27) in the dynamical equation (30) and integrate the linear part of this equation over the transverse variable z and use the reduced quasi-2D model bulk chemical potential (44) in the resultant equation, we obtain the following quasi-2D nonlinear Schrödinger equation for relevant dynamics in the x - y plane for the Bose superfluid along the crossover

$$i \frac{\partial \phi_B^{2D}(x, y, t)}{\partial t} = \left[-\frac{1}{2} \frac{\partial^2}{\partial x^2} - \frac{1}{2} \frac{\partial^2}{\partial y^2} + \frac{1}{2} \lambda^2 x^2 + \frac{1}{2} v^2 y^2 + \mu_B^{2D}(n_B^{2D}, a_B) \right] \phi_B^{2D}(x, y, t), \quad (46)$$

with the normalization $\int dx dy |\phi_B^{2D}(x, y, t)|^2 = 1$. Using the dimensionless space and time variables $\tilde{x} = x/l_B, \tilde{y} = y/l_B, \tilde{t} = t\omega_B$, 2D density as $\tilde{n}_B^{2D} = n_B^{2D} l_B^2$, etc. the quasi-2D nonlinear Schrödinger equation in dimensionless form, is then written as

$$i \frac{\partial \tilde{\phi}_B^{2D}(\tilde{x}, \tilde{y}, \tilde{t})}{\partial \tilde{t}} = \left[-\frac{1}{2} \frac{\partial^2}{\partial \tilde{x}^2} - \frac{1}{2} \frac{\partial^2}{\partial \tilde{y}^2} + \frac{1}{2} \lambda^2 \tilde{x}^2 + \frac{1}{2} v^2 \tilde{y}^2 + \tilde{\mu}_B^{2D}(\tilde{n}_B^{2D}, \tilde{a}_B) \right] \tilde{\phi}_B^{2D}(\tilde{x}, \tilde{y}, \tilde{t}). \quad (47)$$

The transverse dynamics along the integrated z direction is now frozen in the harmonic-oscillator ground state. Using Eq. (44), the dimensionless bulk chemical potential in Eq. (47) along the crossover is given as

$$\tilde{\mu}_B^{2D}(\tilde{n}_B^{2D}, \tilde{a}_B) = \frac{2\sqrt{2\pi}\tilde{\varepsilon} \left[\tilde{a}_B + \frac{2\alpha\sqrt{\tilde{\varepsilon}}\tilde{a}_B^{5/2}}{\sqrt{5\sqrt{\pi}}} \right]}{1 + \frac{\alpha\sqrt{\tilde{\varepsilon}}\tilde{a}_B^{3/2}}{\sqrt{5\sqrt{\pi}}} + \frac{4\sqrt{2\pi}\alpha\pi^{1/12}\tilde{\varepsilon}^{5/6}\tilde{a}_B^{5/2}}{\sqrt{3}\eta_B}}, \quad (48)$$

where $\tilde{\varepsilon} = \sqrt{\gamma}\tilde{n}_B^{2D}$.

4 Quasi-1D and Quasi-2D reduction for fermions

4.1 Quasi-1D configuration

Extending the treatment of the previous section to a fully-paired superfluid Fermi gas at unitarity, in the quasi-1D case, Eqs. (16) and (12), when substituted into Eqs. (24) and (25), lead to the following expressions for the bulk chemical potential and energy density of a

quasi-1D Fermi superfluid mobile along the x direction with tight binding in transverse y and z directions ($v, \gamma \gg \lambda$)

$$\lim_{|a_F| \rightarrow \infty} \mu_F^{1D}(n_F^{1D}, a_F) = \frac{\hbar^2}{m_F} \frac{3\eta_F}{10} \zeta^2, \quad \zeta = \frac{(3\pi n_F^{1D})^{1/3}}{(d_y d_z)^{1/3}}, \quad (49)$$

$$\lim_{|a_F| \rightarrow \infty} \mathcal{E}_F^{1D}(n_F^{1D}, a_F) = \frac{\hbar^2}{m_F} \frac{9\eta_F}{50} \zeta^2, \quad (50)$$

where $\Phi_F^{2D}(y, z)$ is now defined by Eq. (23) with $d_z = l_F/\sqrt{\gamma} = \sqrt{(m_B/m_F)}l_B/\sqrt{\gamma}$, $d_y = l_F/\sqrt{v} = \sqrt{(m_B/m_F)}l_B/\sqrt{v}$ with $l_F = \sqrt{\hbar/(m_F \omega_F)}$, as we take here $\omega_B = \omega_F$. Equations (49) and (50) are fermionic counterparts of bosonic equations (31) and (32).

Similarly, the corresponding equations for the bulk chemical potential and energy density of the paired superfluid fermions in the weak-coupling limit with LHY correction, viz. Eqs. (14) and (10), when substituted into Eqs. (24) and (25), lead to the following expressions for the same quantities in quasi-1D case

$$\mu_F^{1D}(n_F^{1D}, a_F) = \frac{\hbar^2}{m_F} \frac{3}{10} \zeta^2 [1 + f_1 \bar{\zeta} + f_2 \bar{\zeta}^2 + \dots], \quad (51)$$

$$\mathcal{E}_F^{1D}(n_F^{1D}, a_F) = \frac{\hbar^2}{m_F} \frac{9}{50} \zeta^2 [1 + g_1 \bar{\zeta} + g_2 \bar{\zeta}^2 + \dots], \quad (52)$$

where $f_1 = 5d_1/6, f_2 = 5d_2/7, g_1 = 5c_1/6, g_2 = 5c_2/7$, dimensionless $\bar{\zeta} = a_F \zeta$. Equations (49)-(50), on the one hand, valid at unitarity, and Eqs. (51)-(52), on the other hand, valid in the weak-coupling limit, can be combined together to yield the following Padé-type approximants for the weak coupling to unitarity crossover in this case

$$\mu_F^{1D}(n_F^{1D}, a_F) = \frac{\hbar^2}{m_F} \frac{3}{10} \zeta^2 \left[1 + \frac{f_1 \bar{\zeta} + (f_2 - 2f_1^2) \bar{\zeta}^2}{1 - 2f_1 \bar{\zeta} + \frac{(f_2 - 2f_1^2) \bar{\zeta}^2}{\eta_F - 1}} \right], \quad (53)$$

$$\mathcal{E}_F^{1D}(n_F^{1D}, a_F) = \frac{\hbar^2}{m_F} \frac{9}{50} \zeta^2 \left[1 + \frac{g_1 \bar{\zeta} + (g_2 - 2g_1^2) \bar{\zeta}^2}{1 - 2g_1 \bar{\zeta} + \frac{(g_2 - 2g_1^2) \bar{\zeta}^2}{\eta_F - 1}} \right]. \quad (54)$$

For a noninteracting degenerate Fermi gas the quasi-1D chemical potential and energy density obtained by inserting expressions (20) and (19) in Eqs. (24) and (25), respectively, are

$$\mu_F^{1D}(n_F^{1D}) = \frac{\hbar^2}{m_F} \frac{3}{10} \zeta_1^2, \quad \zeta_1 = \frac{(6\pi n_F^{1D})^{1/3}}{(d_y d_z)^{1/3}} \quad (55)$$

$$\mathcal{E}_F^{1D}(n_F^{1D}) = \frac{\hbar^2}{m_F} \frac{9}{50} \zeta_1^2. \quad (56)$$

If we substitute the wave function defined by Eqs. (22) and (23) in the dynamical equation (30) and integrate the linear part of this equation over the transverse variables y and z , following Ref. [50], and use the reduced quasi-1D model bulk chemical potential (53) in the resultant equation, we obtain the following quasi-1D nonlinear Schrödinger equation for relevant dynamics in the x direction for the Fermi superfluid along the crossover, valid between the weak coupling and unitarity limits

$$i\hbar \frac{\partial \phi_F^{1D}(x, t)}{\partial t} = \left[-\frac{\hbar^2}{8m_F} \frac{\partial^2}{\partial x^2} + \frac{1}{2} m_F \omega_F^2 \lambda^2 x^2 + \mu_F^{1D}(n_F^{1D}, a_F) \right] \phi_F^{1D}(x, t), \quad (57)$$

with the normalization $\int dx |\phi_F^{1D}(x, t)|^2 = 1$. To write the dimensionless form of this equation we express lengths in units of $l_B \equiv \sqrt{\hbar/m_B \omega_B}$, time in units of ω_B^{-1} , etc. We are using the bosonic length scale for deriving the dimensionless equations for fermions for future convenience in writing the same for a Bose-Fermi mixture using the same scale. Then the dimensionless quasi-1D nonlinear Schrödinger equation for a superfluid or a degenerate Fermi gas, for the relevant dynamics along the x direction, using the same units as used for bosons, is then written as [39, 41, 70]

$$i \frac{\partial \tilde{\phi}_F^{1D}(\tilde{x}, \tilde{t})}{\partial \tilde{t}} = \left[-\frac{m_B}{8m_F} \frac{\partial^2}{\partial \tilde{x}^2} + \frac{m_F}{2m_B} \lambda^2 \tilde{x}^2 + \tilde{\mu}_F^{1D}(\tilde{n}_F^{1D}, \tilde{a}_F) \right] \tilde{\phi}_F^{1D}(\tilde{x}, \tilde{t}), \quad (58)$$

with the normalization $\int d\tilde{x} |\tilde{\phi}_F^{1D}(\tilde{x}, \tilde{t})|^2 = 1$. The dimensionless crossover formula for the bulk chemical potential of a superfluid Fermi gas, as obtained from Eq. (53) and to be used in Eq. (58), is

$$\tilde{\mu}_F^{1D}(\tilde{n}_F^{1D}, \tilde{a}_F) = \frac{3m_B}{10m_F} \tilde{\zeta}^2 \left[1 + \frac{f_1 \tilde{\zeta} + (f_2 - 2f_1^2) \tilde{\zeta}^2}{1 - 2f_1 \tilde{\zeta} + \frac{(f_2 - 2f_1^2) \tilde{\zeta}^2}{\eta_F^{-1}}} \right], \quad (59)$$

where dimensionless $\tilde{\zeta} = (3\pi \tilde{n}_F^{1D} m_F \sqrt{\gamma V} / m_B)^{1/3}$. In the case of a spin-polarized degenerate Fermi gas, the dimensionless bulk chemical potential to be used in Eq. (58), as obtained from Eq. (55), can be written as

$$\tilde{\mu}_F^{1D}(\tilde{n}_F^{1D}) = \frac{3m_B^{1/3}}{10m_F^{1/3}} (6\pi \tilde{n}_F^{1D} \sqrt{\gamma V})^{2/3}. \quad (60)$$

4.2 Quasi-2D configuration

The bulk chemical potential and energy density for a quasi-2D Fermi superfluid, confined in the x - y plane with tight binding along the z direction ($\gamma \gg v, \lambda$), can be obtained using Eqs. (28) and (29). At unitarity, the bulk chemical potential and energy density, given by Eqs. (16) and (12), respectively, when inserted into Eqs. (28) and (29), lead to the following expressions for these quantities for a quasi-2D Fermi superfluid mobile along the x and y directions

$$\lim_{|a_F| \rightarrow \infty} \mu_F^{2D}(n_F^{2D}, a_F) = \frac{\hbar^2}{m_F} \frac{\sqrt{3}\eta_F}{2\sqrt{5}} \chi^2, \quad (61)$$

$$\lim_{|a_F| \rightarrow \infty} \mathcal{E}_F^{2D}(n_F^{2D}, a_F) = \frac{\hbar^2}{m_F} \frac{3\sqrt{3}\eta_F}{10\sqrt{5}} \chi^2, \quad (62)$$

where $\chi = (3\pi^{3/2} n_F^{2D} / d_z)^{1/3}$. Similarly, the bulk chemical potential and energy density in weakly interacting domain with LHY correction, given by Eqs. (14) and (10), respectively, when substituted in Eqs. (28) and (29), yield the same quantities for a quasi-2D Fermi superfluid:

$$\mu_F^{2D}(n_F^{2D}, a_F) = \frac{\hbar^2}{m_F} \frac{\sqrt{3}}{2\sqrt{5}} \chi^2 [1 + h_1 \tilde{\chi} + h_2 \tilde{\chi}^2 + \dots], \quad (63)$$

$$\mathcal{E}_F^{2D}(n_F^{2D}, a_F) = \frac{3\sqrt{3}\hbar^2}{10\sqrt{5}m_F} \chi^2 [1 + j_1 \tilde{\chi} + j_2 \tilde{\chi}^2 + \dots], \quad (64)$$

where $\bar{\chi} = \chi a_F$, $h_1 = \sqrt{5}d_1/\sqrt{6}$, $h_2 = \sqrt{5}d_2/\sqrt{7}$, $j_1 = \sqrt{5}c_1/\sqrt{6}$, and $j_2 = \sqrt{5}c_2/\sqrt{7}$. Equations (61) and (62), on the one hand, valid at unitarity, and (63) and (64), on the other hand, valid for weak coupling, can be combined together to yield the following crossover formulae valid from weak coupling to unitarity limit for the quasi-2D bulk chemical potential and energy density

$$\mu_F^{2D}(n_F^{2D}, a_F) = \frac{\sqrt{3}\hbar^2}{2\sqrt{5}m_F} \chi^2 \left[1 + \frac{h_1 \bar{\chi} + (h_2 - 2h_1^2) \bar{\chi}^2}{1 - 2h_1 \bar{\chi} + \frac{(h_2 - 2h_1^2) \bar{\chi}^2}{\eta_F - 1}} \right], \quad (65)$$

$$\mathcal{E}_F^{2D}(n_F^{2D}, a_F) = \frac{3\sqrt{3}\hbar^2}{10\sqrt{5}m_F} \chi^2 \left[1 + \frac{j_1 \bar{\chi} + (j_2 - 2j_1^2) \bar{\chi}^2}{1 - 2j_1 \bar{\chi} + \frac{(j_2 - 2j_1^2) \bar{\chi}^2}{\eta_F - 1}} \right]. \quad (66)$$

For a noninteracting degenerate Fermi gas, the quasi-2D chemical potential and energy density obtained by inserting expressions (20) and (19) into Eqs. (28) and (29), respectively, are

$$\mu_F^{2D}(n_F^{2D}) = \frac{\hbar^2}{m_F} \frac{\sqrt{3}}{2\sqrt{5}} \chi_1^2, \quad \chi_1 = \frac{(6\pi^{3/2} n_F^{2D})^{1/3}}{d_z^{1/3}} \quad (67)$$

$$\mathcal{E}_F^{2D}(n_F^{2D}) = \frac{\hbar^2}{m_F} \frac{3\sqrt{3}}{10\sqrt{5}} \chi_1^2. \quad (68)$$

Following the same procedure as above, integrating out the transverse z variable, the dimensionless quasi-2D nonlinear Schrödinger equation for a superfluid or a degenerate Fermi gas, for the relevant dynamics in the x - y plane, using the same units as used for bosons, is then written as [39, 41, 70]

$$i \frac{\partial \tilde{\phi}_F^{2D}(\tilde{x}, \tilde{y}, \tilde{t})}{\partial \tilde{t}} = \left[-\frac{m_B}{8m_F} \left(\frac{\partial^2}{\partial \tilde{x}^2} + \frac{\partial^2}{\partial \tilde{y}^2} \right) + \frac{m_F}{2m_B} (\lambda^2 \tilde{x}^2 + v^2 \tilde{y}^2) + \tilde{\mu}_F^{2D}(\tilde{n}_F^{2D}, \tilde{a}_F) \right] \tilde{\phi}_F^{2D}(\tilde{x}, \tilde{y}, \tilde{t}), \quad (69)$$

with the normalization $\int d\tilde{x}d\tilde{y} |\tilde{\phi}_F^{2D}(\tilde{x}, \tilde{y}, \tilde{t})|^2 = 1$, here the dimensionless bulk chemical potential $\tilde{\mu}_F^{2D}(\tilde{n}_F^{2D}, \tilde{a}_F)$ is given by

$$\tilde{\mu}_F^{2D}(\tilde{n}_F^{2D}, \tilde{a}_F) = \frac{\sqrt{3}m_B}{2\sqrt{5}m_F} \tilde{\chi}^2 \left[1 + \frac{h_1 \tilde{\chi} + (h_2 - 2h_1^2) \tilde{\chi}^2}{1 - 2h_1 \tilde{\chi} + \frac{(h_2 - 2h_1^2) \tilde{\chi}^2}{\eta_F - 1}} \right], \quad (70)$$

where dimensionless $\tilde{\chi} = (3\pi^{3/2} \tilde{n}_F^{2D} \sqrt{\gamma m_F/m_B})^{1/3}$. For a degenerate Fermi gas Eq. (69) remains valid but with the bulk chemical potential of Eq. (67) expressed in dimensionless units

$$\tilde{\mu}_F^{2D}(\tilde{n}_F^{2D}) = \frac{\sqrt{3}\pi m_B^{2/3}}{2\sqrt{5}m_F^{2/3}} (6\tilde{n}_F^{2D} \sqrt{\gamma})^{2/3}. \quad (71)$$

5 Model equations for 3D, quasi-1D, and quasi-2D Bose-Fermi superfluid mixtures

The dynamical equations for an uncoupled Bose-Fermi superfluid or degenerate mixture (without interspecies interaction) can readily be written by combining the Bose and Fermi equations of Secs. 3 and 4. We will now consider a weakly interacting Bose-Fermi mixture. For a Bose-Fermi superfluid mixture, the 3D interspecies energy density takes the following form in dimensionless units

$$\tilde{\mathcal{E}}_{BF} = \frac{2\pi\tilde{a}_{BF}}{\xi} |\tilde{\phi}_B^{3D}|^2 |\tilde{\phi}_F^{3D}|^2, \quad (72)$$

where $\xi = m_F/(m_B + m_F)$ and \tilde{a}_{BF} is the Bose-Fermi interspecies scattering length in dimensionless units. The full 3D model Bose-Fermi equations in dimensionless units are

$$i \frac{\partial \tilde{\phi}_B^{3D}(\tilde{\mathbf{r}}, \tilde{t})}{\partial \tilde{t}} = \left[-\frac{1}{2} \nabla^2 + \frac{\lambda^2 \tilde{x}^2 + \nu^2 \tilde{y}^2 + \gamma^2 \tilde{z}^2}{2} + \tilde{U}_{12} |\tilde{\phi}_F^{3D}|^2 \right. \\ \left. + \frac{4\pi\tilde{n}_B^{2/3} (\tau + \alpha\tau^{5/2})}{1 + \frac{\alpha}{2}\tau^{3/2} + \frac{4\pi\alpha}{\eta_B}\tau^{5/2}} \right] \tilde{\phi}_B^{3D}(\tilde{\mathbf{r}}, \tilde{t}), \quad (73)$$

$$i \frac{\partial \tilde{\phi}_F^{3D}(\mathbf{r}, t)}{\partial \tilde{t}} = \left[-\frac{m_B}{8m_F} \nabla^2 + \frac{m_F}{2m_B} (\lambda^2 \tilde{x}^2 + \nu^2 \tilde{y}^2 + \gamma^2 \tilde{z}^2) + \tilde{U}_{21} |\tilde{\phi}_B^{3D}|^2 + \frac{m_B(3\pi^2\tilde{n}_F)^{2/3}}{2m_F} \right. \\ \left. \times \left\{ 1 + \frac{d_1 \kappa + (d_2 - 2d_1^2) \kappa^2}{1 - 2d_1 \kappa + \frac{(d_2 - 2d_1^2) \kappa^2}{\eta_F - 1}} \right\} \right] \tilde{\phi}_F^{3D}(\tilde{\mathbf{r}}, \tilde{t}), \quad (74)$$

with normalization $\int |\tilde{\phi}_i^{3D}(\mathbf{r}, t)|^2 d\mathbf{r} = 1$, $\tilde{n}_i = N_i |\tilde{\phi}_i^{3D}|^2$, and where $\tilde{U}_{12} = 2\pi\tilde{a}_{BF}N_F/\xi$, $\tilde{U}_{21} = 2\pi\tilde{a}_{BF}N_B/\xi$.

For a degenerate Fermi gas (74) becomes

$$i \frac{\partial \tilde{\phi}_F^{3D}(\mathbf{r}, t)}{\partial \tilde{t}} = \left[-\frac{m_B}{8m_F} \nabla^2 + \frac{m_F}{2m_B} (\lambda^2 \tilde{x}^2 + \nu^2 \tilde{y}^2 + \gamma^2 \tilde{z}^2) \right. \\ \left. + \tilde{U}_{21} |\tilde{\phi}_B^{3D}|^2 + \frac{m_B(6\pi^2\tilde{n}_F)^{2/3}}{2m_F} \right] \tilde{\phi}_F^{3D}(\tilde{\mathbf{r}}, \tilde{t}). \quad (75)$$

For a Bose-Fermi superfluid mixture, quasi-1D and quasi-2D interspecies energy densities in the weak-coupling limit in dimensionless units can be written as

$$\tilde{\mathcal{E}}_{BF}^{1D} = \frac{2\pi\tilde{a}_{BF}}{\xi} |\tilde{\phi}_B^{1D}(\tilde{x})|^2 |\tilde{\phi}_F^{1D}(\tilde{x})|^2 \int |\tilde{\Phi}_B^{2D}(\tilde{y}, \tilde{z})|^2 |\tilde{\Phi}_F^{2D}(\tilde{y}, \tilde{z})|^2 d\tilde{y}d\tilde{z}, \\ = 2\tilde{a}_{BF} \sqrt{\nu\gamma} |\tilde{\phi}_B^{1D}(\tilde{x})|^2 |\tilde{\phi}_F^{1D}(\tilde{x})|^2, \quad (76)$$

$$\tilde{\mathcal{E}}_{BF}^{2D} = \frac{2\pi\tilde{a}_{BF}}{\xi} |\tilde{\phi}_B^{2D}(\tilde{x}, \tilde{y})|^2 |\tilde{\phi}_F^{2D}(\tilde{x}, \tilde{y})|^2 \int |\tilde{\Phi}_B^{1D}(\tilde{z})|^2 |\tilde{\Phi}_F^{1D}(\tilde{z})|^2 d\tilde{z}, \\ = \frac{2\sqrt{\pi}\tilde{\gamma}\tilde{a}_{BF}}{\sqrt{\xi}} |\tilde{\phi}_B^{2D}(\tilde{x}, \tilde{y})|^2 |\tilde{\phi}_F^{2D}(\tilde{x}, \tilde{y})|^2, \quad (77)$$

where dimensionless $\tilde{\Phi}_B^{2D}(\tilde{y}, \tilde{z})$, $\tilde{\Phi}_F^{2D}(\tilde{y}, \tilde{z})$ and $\tilde{\Phi}_B^{1D}(\tilde{z})$, $\tilde{\Phi}_F^{1D}(\tilde{z})$ are defined as

$$\tilde{\Phi}_B^{2D}(\tilde{y}, \tilde{z}) = \left(\frac{\gamma\nu}{\pi^2} \right)^{1/4} e^{-\gamma\tilde{z}^2/2} e^{-\nu\tilde{y}^2/2}, \quad (78)$$

$$\tilde{\Phi}_F^{2D}(\tilde{y}, \tilde{z}) = \left(\frac{\gamma v m_F^2}{\pi^2 m_B^2} \right)^{1/4} e^{-\gamma m_F \tilde{z}^2 / (2m_B)} e^{-v m_F \tilde{y}^2 / (2m_B)}, \quad (79)$$

$$\tilde{\Phi}_B^{1D}(\tilde{z}) = \left(\frac{\gamma}{\pi} \right)^{1/4} e^{-\gamma \tilde{z}^2 / 2}, \quad (80)$$

$$\tilde{\Phi}_F^{1D}(\tilde{z}) = \left(\frac{\gamma m_F}{\pi m_B} \right)^{1/4} e^{-\gamma m_F \tilde{z}^2 / (2m_B)}. \quad (81)$$

Using these interspecies energy densities, the coupled non-linear Schrödinger equations for the quasi-1D Bose-Fermi superfluid mixture, where the intraspecies Bose and Fermi interactions can be varied from weak-coupling to unitarity limits, can now be written in dimensionless form as

$$i \frac{\partial \tilde{\Phi}_B^{1D}(\tilde{x}, t)}{\partial t} = \left[-\frac{1}{2} \frac{\partial^2}{\partial \tilde{x}^2} + \frac{\lambda^2 \tilde{x}^2}{2} + \tilde{\mu}_B^{1D}(\tilde{n}_B^{1D}, \tilde{a}_B) + \tilde{U}_{12}^{1D} |\tilde{\Phi}_F^{1D}|^2 \right] \tilde{\Phi}_B^{1D}(\tilde{x}, t), \quad (82)$$

$$i \frac{\partial \tilde{\Phi}_F^{1D}(\tilde{x}, t)}{\partial t} = \left[-\frac{m_B \partial^2}{8m_F \partial \tilde{x}^2} + \frac{m_F \lambda^2 \tilde{x}^2}{m_B} + \tilde{\mu}_F^{1D}(\tilde{n}_F^{1D}, \tilde{a}_F) + \tilde{U}_{21}^{1D} |\tilde{\Phi}_B^{1D}|^2 \right] \tilde{\Phi}_F^{1D}(\tilde{x}, t), \quad (83)$$

where $\tilde{U}_{12}^{1D} = 2\tilde{a}_{BF} N_F \sqrt{v\gamma}$ and $\tilde{U}_{21}^{1D} = 2\tilde{a}_{BF} N_B \sqrt{v\gamma}$. The corresponding equations for quasi-2D system are

$$i \frac{\partial \tilde{\Phi}_B^{2D}(\tilde{x}, \tilde{y}, t)}{\partial t} = \left[-\frac{1}{2} \left(\frac{\partial^2}{\partial \tilde{x}^2} + \frac{\partial^2}{\partial \tilde{y}^2} \right) + \frac{\lambda^2 \tilde{x}^2 + v^2 \tilde{y}^2}{2} \right. \\ \left. + \tilde{\mu}_B^{2D}(\tilde{n}_B^{2D}, \tilde{a}_B) + \tilde{U}_{12}^{2D} |\tilde{\Phi}_F^{2D}|^2 \right] \tilde{\Phi}_B^{2D}(\tilde{x}, \tilde{y}, t), \quad (84)$$

$$i \frac{\partial \tilde{\Phi}_F^{2D}(\tilde{x}, \tilde{y}, t)}{\partial t} = \left[-\frac{m_B}{8m_F} \left(\frac{\partial^2}{\partial \tilde{x}^2} + \frac{\partial^2}{\partial \tilde{y}^2} \right) + \frac{m_F}{2m_B} (\lambda^2 \tilde{x}^2 + v^2 \tilde{y}^2) \right. \\ \left. + \tilde{\mu}_F^{2D}(\tilde{n}_F^{2D}, \tilde{a}_F) + \tilde{U}_{21}^{2D} |\tilde{\Phi}_B^{2D}|^2 \right] \tilde{\Phi}_F^{2D}(\tilde{x}, \tilde{y}, t), \quad (85)$$

where $\tilde{U}_{12}^{2D} = 2\sqrt{\pi\gamma/\xi} \tilde{a}_{BF} N_F$ and $\tilde{U}_{21}^{2D} = 2\sqrt{\pi\gamma/\xi} \tilde{a}_{BF} N_B$. Equations (82)-(83) and (84)-(85) with the bulk chemical potentials $\mu_i^{1D}(\tilde{n}_i^{1D}, \tilde{a}_i)$ and $\mu_i^{2D}(\tilde{n}_i^{2D}, \tilde{a}_i)$ given by (39) and (59), and (48) and (70), respectively, are the principal results of this paper valid for quasi-1D and quasi-2D Bose-Fermi mixtures. For a degenerate Fermi gas, these chemical potentials are given by Eqs. (60) and (71), respectively. There are no fitting parameters in these equations; the only parameters in these equations are the universal Bertsch parameter [51] at unitarity and the constants of the LHY interaction [47–49]. Other weak coupling to unitarity crossover models for the Bose-Fermi mixture, in addition, have fitting parameters [31–35, 37, 39, 70], specially for the quasi-1D and quasi-2D configurations.

6 Numerical results

We solve the nonlinear partial differential equations for the Bose-Fermi mixtures of Sec. 5 numerically, by the split-time-step Crank-Nicolson method employing the imaginary-time propagation [71], using C/Fortran programs [72, 73]. We compare the numerical results for reduced 1D densities defined by

$$|\tilde{\Phi}_i^{3D,R}(\tilde{x})|^2 \equiv \int d\tilde{y} d\tilde{z} |\tilde{\Phi}_i^{3D}(\tilde{\mathbf{r}})|^2, \quad (86)$$

$$|\tilde{\Phi}_i^{2D,R}(\tilde{x})|^2 \equiv \int d\tilde{y} |\tilde{\Phi}_i^{2D}(\tilde{x}, \tilde{y})|^2, \quad (87)$$

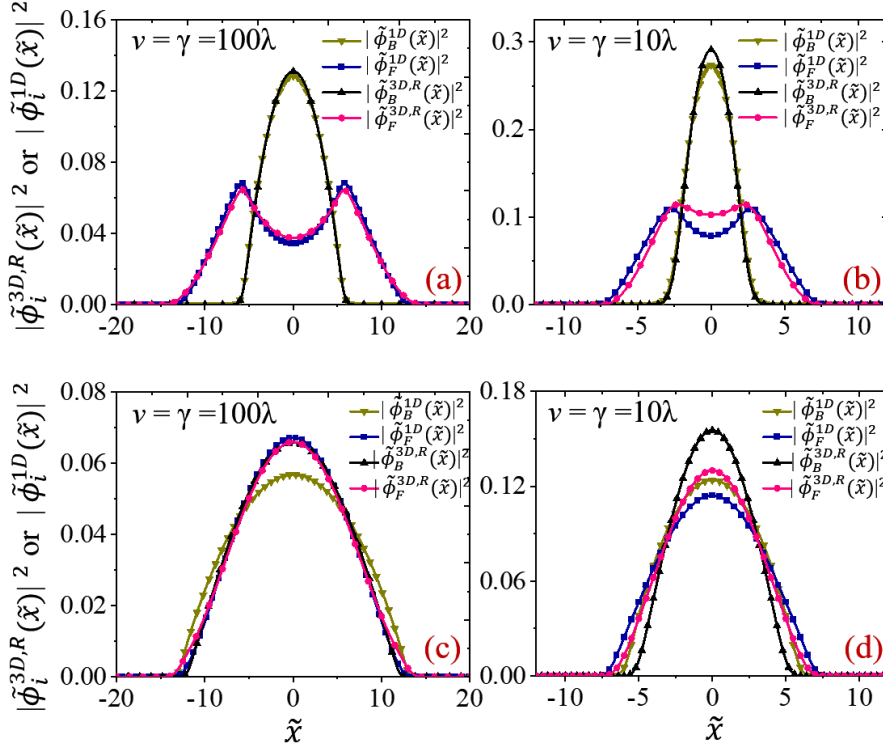


Fig. 1 (Color online) Quasi-1D density $|\tilde{\phi}_i^{1D}(\tilde{x})|^2$ of ${}^7\text{Li}$ - ${}^6\text{Li}$ Bose-Fermi superfluid mixture obtained by solving the quasi-1D Eqs. (82)-(83) compared with the reduced 1D density $|\tilde{\phi}_i^{3D,R}(\tilde{x})|^2$ of Eq. (86) obtained by solving the 3D Eqs. (73)-(74) for $N_B = 1000$, $N_F = 100$, $a_{BF} = 100a_0$, $a_F = -20000a_0$ and with (a) $\omega_i = \omega_x = 2\pi$ Hz, $\lambda = 1$, $v = \gamma = 100$, $a_B = 50a_0$, (b) $\omega_i = \omega_x = 2\pi$ Hz, $\lambda = 1$, $v = \gamma = 10$, $a_B = 50a_0$, (c) $\omega_i = \omega_x = 2\pi$ Hz, $\lambda = 1$, $v = \gamma = 100$, $a_B = 500a_0$, and (d) $\omega_i = \omega_x = 2\pi$ Hz, $\lambda = 1$, $v = \gamma = 10$, $a_B = 500a_0$. The units of \tilde{x} and densities are $38 \mu\text{m}$ and $0.03 \mu\text{m}^{-1}$, respectively.

as appropriate, calculated with quasi-1D, quasi-2D, and full 3D models, viz. (82-83), (84-85), and (73-75), respectively. We will present results for different Bose-Fermi systems of experimental interest, e.g. ${}^7\text{Li}$ - ${}^6\text{Li}$ and ${}^{133}\text{Cs}$ - ${}^6\text{Li}$.

For a strong Bose-Fermi repulsion, there could be a phase separation between the two components of a Bose-Fermi mixture [74]. A symmetric phase separation is characterized by a maximum in the density of one of the components coinciding with the local minimum in the density of the other component at the center of the trap. Such phase separation can occur in both quasi-1D and quasi-2D configurations, which we elaborate next for a superfluid Bose-Fermi mixture. In this paper we use the following values of the Berstch parameters for bosons and fermions, respectively, $\eta_B = 4.7$, $\eta_F = 0.415$ [41]. The Bose parameter is taken from a fit to a realistic Hartree calculation [75], whereas the Fermi parameter is taken from a fit to realistic Monte-Carlo calculations [58, 76, 77] and experiments [78-80].

Trapped quasi-1D Bose-Fermi mixture: We consider a ${}^7\text{Li}$ - ${}^6\text{Li}$ Bose-Fermi superfluid binary mixture with $N_B = 1000$, $N_F = 100$, $a_B = 50a_0$, $a_F = -20000a_0$, and $a_{BF} = 100a_0$, where a_0 is the Bohr radius, in two different trapping potentials: one with $\omega_i = 2\pi$ Hz, $\lambda =$

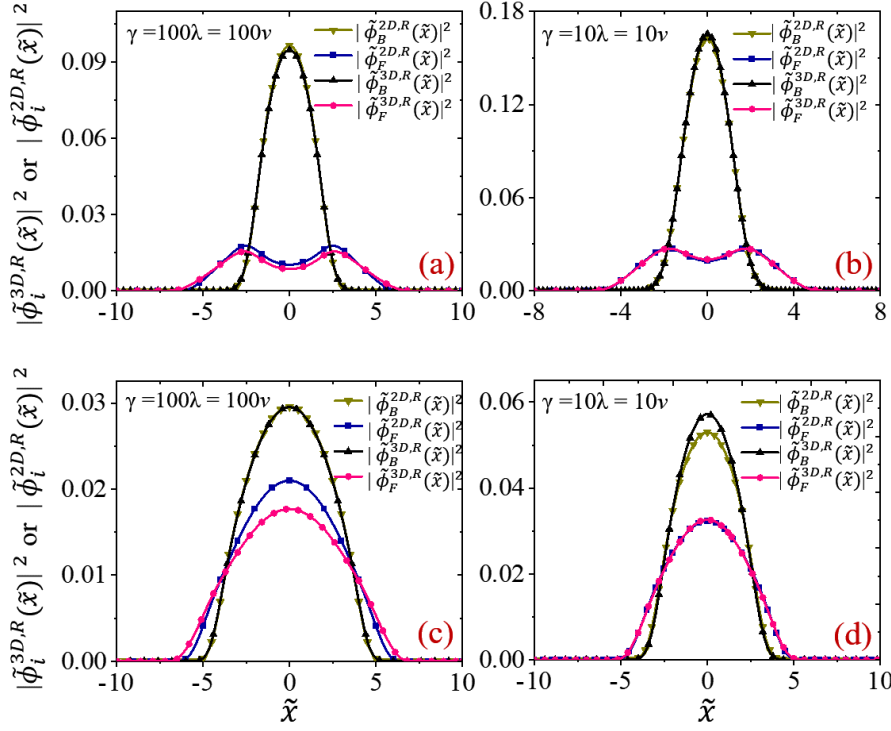


Fig. 2 (Color online) Reduced 1D density $|\tilde{\phi}_i^{2D,R}(\tilde{x})|^2$, viz. Eq. (87), of ${}^7\text{Li}$ - ${}^6\text{Li}$ Bose-Fermi superfluid mixture obtained by solving the quasi-2D Eqs. (84)-(85) and the reduced 1D density $|\tilde{\phi}_i^{3D,R}(\tilde{x})|^2$ of Eq. (86) obtained by solving 3D Eqs. (73)-(74) for $N_B = 1000$, $N_F = 100$, $a_{BF} = 100a_0$, $a_F = -20000a_0$ and with (a) $\omega_i = \omega_x = 2\pi$ Hz, $\lambda = \nu = 1$, $\gamma = 100$, $a_B = 50a_0$, (b) $\omega_i = \omega_x = 2\pi$ Hz, $\lambda = \nu = 1$, $\gamma = 10$, $a_B = 50a_0$. (c) $\omega_i = \omega_x = 2\pi$ Hz, $\lambda = \nu = 1$, $\gamma = 100$, $a_B = 500a_0$, and (d) $\omega_i = \omega_x = 2\pi$ Hz, $\lambda = \nu = 1$, $\gamma = 10$, $a_B = 500a_0$. The units of \tilde{x} and densities are $38 \mu\text{m}$ and $0.03 \mu\text{m}^{-1}$, respectively.

1, $\nu = \gamma = 100$ and the other with $\omega_i = 2\pi$ Hz, $\lambda = 1$, $\nu = \gamma = 10$ in (21). The up-down Fermi-Fermi interaction is taken to be near the unitarity limit. In this system, we compare the quasi-1D density $|\phi_i^{1D}(\tilde{x})|^2$ obtained by solving the quasi-1D Bose-Fermi equations (82)-(83) with the reduced 1D density (86) obtained by solving the 3D Bose-Fermi equations (73)-(74). The respective densities are plotted in Fig. 1 for (a) $\nu = \gamma = 100\lambda$, and (b) $\nu = \gamma = 10\lambda$. Although there is good agreement between the two densities in both cases, the agreement between the two is better in (a) than in (b), as in the former case a stronger transverse trap creates a more ideal quasi-1D confinement than in the latter. In this case, the system shows a phase separation [74] between the two components. For the same set of parameters, if we keep on increasing the Bose-Bose repulsion by increasing a_B , then the mixture enters into the miscible domain. We illustrate this for $a_B = 500a_0$ in two different trapping potentials: $\omega_i = \omega_x = 2\pi$ Hz, $\lambda = 1$, $\nu = \gamma = 100$ in Fig. 1(c) and $\omega_i = \omega_x = 2\pi$ Hz, $\lambda = 1$, $\nu = \gamma = 10$ in Fig. 1(d). Again, the agreement between the two densities is better in Fig. 1(c) with a stronger transverse trap.

Trapped quasi-2D Bose-Fermi mixture: In this case, we again consider a ${}^7\text{Li}$ - ${}^6\text{Li}$ Bose-Fermi superfluid mixture with $N_B = 1000$, $N_F = 100$, $a_B = 50a_0$, $a_F = -20000a_0$, $a_{BF} =$

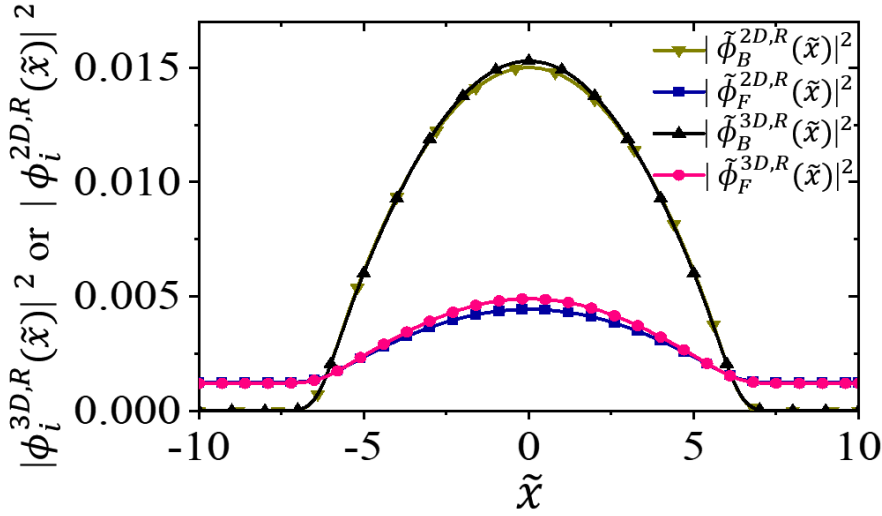


Fig. 3 (Color online) Reduced 1D density $|\phi_i^{2D,R}(\tilde{x})|^2$, viz. Eq. (87), of bosons and fermions in a quasi-2D Bose-Fermi mixture obtained by solving the quasi-2D equations (84)-(85) compared with reduced 1D density $|\phi_i^{3D,R}(\tilde{x})|^2$, viz. Eq. (86), obtained by solving the 3D equations (73)-(74) for $N_B = 20000$, $N_F = 100$, $a_B = 230a_0$, $a_{BF} = -100a_0$ and $a_F = 0^-$. The BEC in the mixture is confined in a harmonic trapping potential with $\omega_B = 2\pi$ Hz, $\nu = \lambda = 1$, $\gamma = 100$, whereas Fermi superfluid is confined only along z direction with $\omega_F = 2\pi$ Hz, $\nu = \lambda = 0$, $\gamma = 100$. The units of \tilde{x} and densities are $8.7 \mu\text{m}$ and $0.115 \mu\text{m}^{-1}$, respectively.

$100a_0$ in two different trapping potentials: $\omega_i = 2\pi$ Hz, $\lambda = \nu = 1$, $\gamma = 100$ and $\omega_i = 2\pi$ Hz, $\lambda = \nu = 1$, $\gamma = 10$ in Eq. (21). In this system, we compare the reduced 1D density $|\phi_i^{2D,R}(\tilde{x})|^2$ of Eq. (87) obtained by solving the quasi-2D Bose-Fermi equations (84)-(85) with the reduced 1D density $|\phi_i^{3D,R}(\tilde{x})|^2$ of Eq. (86) obtained by solving the 3D Bose-Fermi equations (73)-(74). The respective densities are plotted in figure 2 for (a) $\gamma = 100\nu = 100\lambda$, and (b) $\gamma = 10\nu = 10\lambda$. A minimum of the Fermi density at the center in these cases signals a phase separation between the two components. The agreement between the two densities is good in both cases.

Again for a sufficiently increased Bose-Bose repulsion, the mixture is in the miscible domain. We exhibit the miscible phase for $a_B = 500a_0$ in two different trapping potentials: $\omega_i = 2\pi$ Hz, $\lambda = \nu = 1$, $\gamma = 100$ in Fig. 2(c) and $\omega_i = 2\pi$ Hz, $\lambda = \nu = 1$, $\gamma = 10$ in Fig. 2(d). The densities obtained from the quasi-2D equation are found to be a better approximation to the same densities obtained from the 3D equation, viz. figure 2, while the densities obtained from the quasi-1D equation may lead to a less accurate approximation when compared to the same obtained from the 3D equation, viz. figure 1, not only in the present Bose-Fermi mixture but also in the case of a single-component BEC [50].

In two elegant experiments [18, 19] Desalvo *et al.* demonstrated that an attractive interspecies interaction in a degenerate Bose-Fermi mixture leads to an effective attraction between the bosonic (fermionic) atoms created by the presence of the fermionic (bosonic) atoms. This effective attraction may trap bosonic [19] (fermionic [18]) atoms in a trapped Fermi (Bose) gas under favorable conditions. We show that similar trapping is also possible in a superfluid Bose-Fermi mixture for parameters very similar to those used in these experiments and we consider this possibility first in the following.

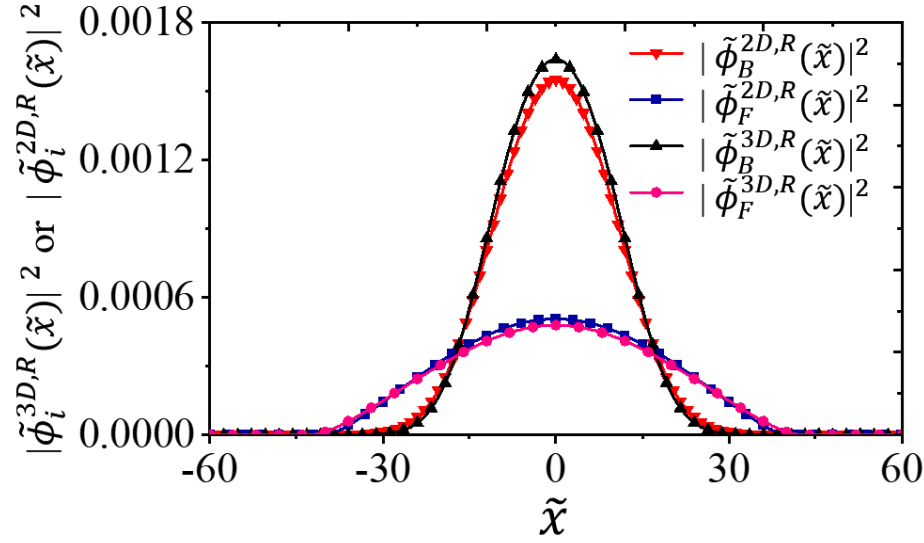


Fig. 4 (Color online) Reduced 1D density $|\phi_i^{2D,R}(\tilde{x})|^2$, viz. Eq. (87), of bosons and fermions in a quasi-2D Bose-Fermi mixture obtained by solving the quasi-2D equations (84)-(85) compared with reduced 1D density $|\phi_i^{3D,R}(\tilde{x})|^2$, viz. Eq. (86), obtained by solving the 3D equations (73)-(74) for $N_B = 5000$, $N_F = 500$, $a_B = 3a_0$, $a_{BF} = -100a_0$ and $a_F = 0^-$. The Fermi superfluid in the mixture is confined by a harmonic trapping potential with $\omega_F = 2\pi$ Hz, $\nu = \lambda = 1$, $\gamma = 100$, whereas the BEC is confined only along z direction with $\omega_B = 2\pi$ Hz, $\nu = \lambda = 0$, $\gamma = 100$. The units of \tilde{x} and densities are $8.7 \mu\text{m}$ and $0.115 \mu\text{m}^{-1}$, respectively.

Trapping of a Bose (Fermi) superfluid by a Fermi (Bose) superfluid by fermion- (boson-) mediated interaction: To study the trapping of free Fermi superfluid in a trapped BEC, we consider a ^{133}Cs - ^6Li Bose-Fermi superfluid mixture, where the spin-up-down fermionic ^6Li atoms are interacting via s -wave scattering length $a_F \rightarrow 0^-$. The mixture has an interspecies Feshbach resonance around 893 Gauss that tunes the interaction between ^6Li and ^{133}Cs [18]. Across this resonance, a_B varies from $220a_0$ to $280a_0$, and we have chosen $a_B = 230a_0$. For the Bose gas-mediated trapping of Fermi superfluid, we vary a_{BF} to the requisite values and atoms of both species are mixed in a certain proportion. In accordance with the experiment by Desalvo *et al.* [18], we consider the harmonically-trapped ^{133}Cs BEC with angular trap frequencies $\omega_x = \omega_y = 2\pi$ Hz, and $\omega_z = 2\pi \times 100$ Hz, whereas the fermionic component is supposed to be harmonically trapped only along the z direction with angular trap frequency $\omega_z = 2\pi \times 100$ Hz and free in the x - y plane. As an example, we show the trapping of 100 ^6Li atoms with $a_F \rightarrow 0^-$ by a BEC consisting of 20000 atoms of ^{133}Cs interacting with the Fermi superfluid via a Bose-Fermi scattering length $a_{BF} = -100a_0$. Due to the Pauli exclusion principle, only a limited number of fermions can be trapped. In Fig. 3 we plot the reduced 1D densities $|\phi_i^{2D,R}(\tilde{x})|^2$ of Eq. (87) of the two components as calculated from a solution of the quasi-2D equations (84) and (85) and compare these with the reduced 1D densities $|\phi_i^{3D,R}(\tilde{x})|^2$ of Eq. (86) obtained by solving the 3D Bose-Fermi equations (73)-(74) in Fig. 3.

Similarly, to study the trapping of bosonic atoms in a trapped Fermi superfluid, we again consider a ^{133}Cs - ^6Li Bose-Fermi superfluid mixture, where the spin-up-down fermionic ^6Li atoms are interacting via s -wave scattering length $a_F \rightarrow 0^-$. The fermionic ^6Li atoms are

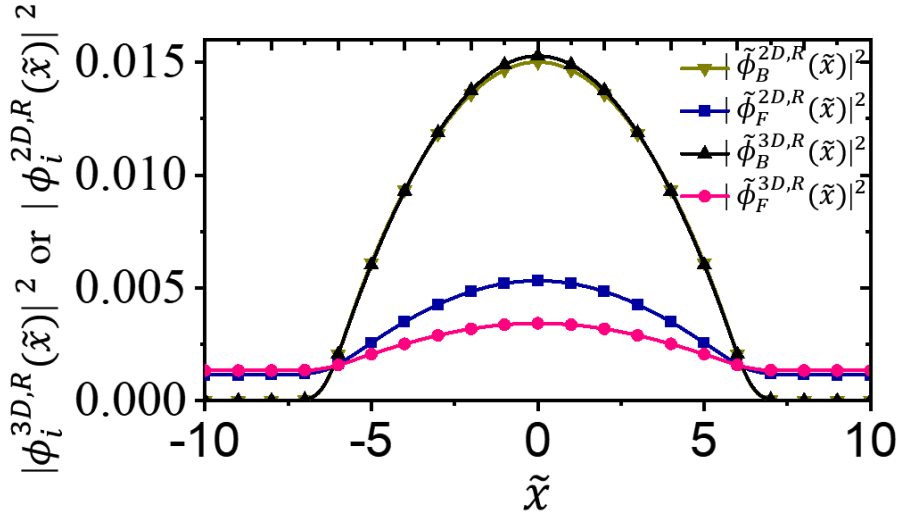


Fig. 5 (Color online) Reduced 1D density $|\phi_i^{2D,R}(\tilde{x})|^2$, viz. (87), of bosons and fermions in a quasi-2D degenerate Bose-Fermi mixture obtained by solving the quasi-2D equations (84)-(85) compared with reduced 1D density $|\phi_i^{3D,R}(\tilde{x})|^2$, viz. (86), obtained by solving the 3D equations (73) and (75) for $N_B = 20000$, $N_F = 100$, $a_B = 230a_0$, $a_{BF} = -100a_0$. The BEC in the mixture is confined by a harmonic trapping potential with $\omega_B = 2\pi$ Hz, $\nu = \lambda = 1$, $\gamma = 100$, whereas degenerate Fermi gas is confined only along z direction with $\omega_F = 2\pi$ Hz, $\nu = \lambda = 0$, $\gamma = 100$. The units of \tilde{x} and densities are $8.7 \mu\text{m}$ and $0.115 \mu\text{m}^{-1}$, respectively.

harmonically trapped with angular frequencies $\omega_x = \omega_y = 2\pi$ Hz, and $\omega_z = 2\pi \times 100$ Hz, whereas the bosonic ^{133}Cs atoms are harmonically-confined along the z direction with angular frequency $\omega_z = 2\pi \times 100$ Hz and free in the x - y plane. We show that with attractive interspecies interaction characterized by $a_{BF} = -100a_0$ the BEC turns out to be self-trapped in x - y plane too as is illustrated in figure 4, where we plot the reduced densities (87) of the two components as calculated from a solution of the quasi-2D equations (84) and (85) and compared these with the reduced densities $|\phi_i^{3D,R}(\tilde{x})|^2$ in Eq. (86) obtained by solving the 3D Bose-Fermi equations (73-74). In both Figs. 3 and 4, the densities obtained from a solution of quasi-2D model are in reasonable agreement with those obtained from the 3D model for Bose-Fermi superfluid mixtures.

Finally, we consider the trapping of the Bose (Fermi) component by the interaction mediated by the Fermi (Bose) component in a ^{133}Cs - ^6Li Bose-Fermi degenerate mixture exactly as in the experiments of Desalvo *et al.* [18]. The bosons are in a superfluid state whereas the fermions in a degenerate spin-polarized state. We present results for reduced 1D densities of a degenerate Bose-Fermi mixture in Figs. 5 and 6 obtained from a solution the quasi-2D Bose-Fermi equations (84)-(85) and compare these with a solution of the 3D Bose-Fermi equations (73) and (74) using exactly the same parameters as in Figs. 3 and 4 for the ^{133}Cs - ^6Li Bose-Fermi superfluid mixture. For the degenerate mixture, the bulk chemical potentials for fermions are given by Eq. (71) for the quasi-2D case and by Eq. (20) for the 3D case. If we compare Figs. 3 and 5, both with $N_B = 20000$ and $N_F = 100$, we note that these systems are essentially bosonic with a small fermionic part. Consequently, the bosonic density in both cases are practically the same with a small change in the fermionic density. In Figs. 4 and 6, both with $N_B = 5000$ and $N_F = 500$, although the number of bosons is larger

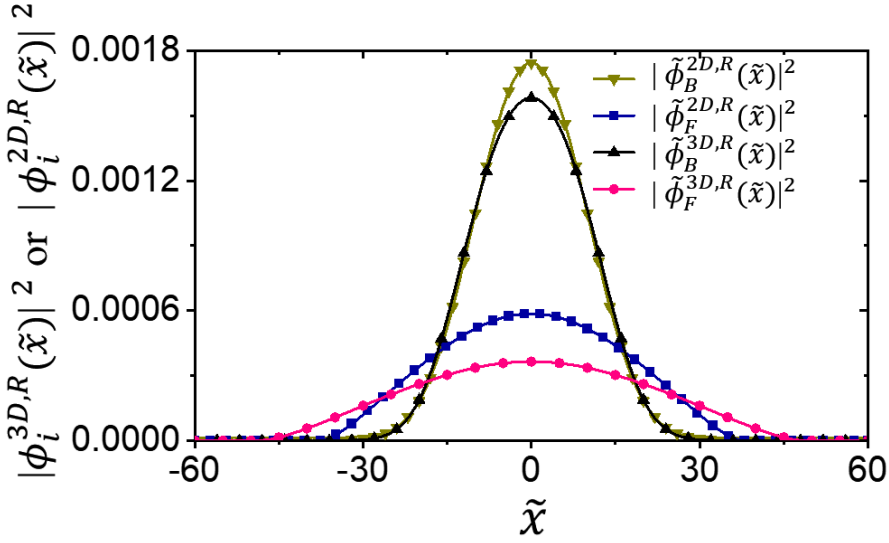


Fig. 6 (Color online) Reduced 1D density $|\phi_i^{2D,R}(\tilde{x})|^2$, viz. (87), of bosons and fermions in a quasi-2D Bose-Fermi mixture obtained by solving the quasi-2D equations (84)-(85) compared with reduced 1D density $|\phi_i^{3D,R}(\tilde{x})|^2$, viz. (86), obtained by solving the 3D equations (73) and (75) for $N_B = 5000$, $N_F = 500$, $a_B = 3a_0$, $a_{BF} = -100a_0$. The degenerate Fermi gas in the mixture is confined by a harmonic trapping potential with $\omega_F = 2\pi$ Hz, $v = \lambda = 1$, $\gamma = 100$, whereas the BEC is confined only along z direction with $\omega_B = 2\pi$ Hz, $v = \lambda = 0$, $\gamma = 100$. The units of \tilde{x} and densities are $8.7 \mu\text{m}$ and $0.115 \mu\text{m}^{-1}$, respectively.

than the number of fermions, the latter is not negligible. Consequently, both densities have changed in the degenerate Fermi case. The reduced 1D densities obtained from the quasi-2D model in the superfluid Fermi case is a better approximation to the reduced 1D densities obtained from the 3D model, viz. Fig. 4 when compared to the same in the degenerate Fermi gas case, viz. Fig. 6.

7 SUMMARY

We have formulated dynamical equations for quasi-1D and quasi-2D superfluid and also degenerate Bose-Fermi mixtures for the weak coupling to unitarity crossover without any fitting parameters; the only parameters of the model are the constants of the beyond-mean-field LHY interactions for bosons and fermions [47–49] and the universal Bertsch parameter [51] at unitarity. We tested these numerically in a few problems of superfluid Bose-Fermi mixture confined by quasi-1D and quasi-2D traps. First we considered the problem of phase-separated and miscible Bose-Fermi mixture where both components are subject either to a quasi-1D trap or a quasi-2D trap. We also considered the problem of self-trapping of one of the components in the other trapped component in a quasi-2D Bose-Fermi superfluid as well as in a degenerate Bose-Fermi mixture. Here the first component is subjected to a quasi-2D trap, whereas the self-trapped second component is subjected to a trap only in the z direction. In both cases – the problem of phase separation and of self-trapping of one of the components by the other – we found that the densities obtained from the quasi-1D and

quasi-2D model equations are in good agreement with the densities obtained from a solution of the full 3D model.

Acknowledgments

S.G. acknowledges the support of the Science and Engineering Research Board (SERB), Department of Science and Technology, Government of India under the project CRG/2021/002597. S.K.A. acknowledges support by Conselho Nacional de Desenvolvimento Científico e Tecnológico (CNPq), Brazil under grant 301324/2019-0.

Data Availability

Data Availability Statement: No Data associated in the manuscript.

References

1. G. Modugno, M. Modugno, F. Riboli, G. Roati, M. Inguscio, *Phys. Rev. Lett.* **89**, 190404 (2002).
2. S. B. Papp, J. M. Pino, C. E. Wieman, *Phys. Rev. Lett.* **101**, 040402 (2008).
3. K. E. Wilson, A. Guttridge, J. Segal, S. L. Cornish, *Phys. Rev. A* **103**, 033306 (2021).
4. X. Cui, Y. Ma, *Phys. Rev. Research* **3**, L012027 (2021).
5. H. Pu, N. P. Bigelow, *Phys. Rev. Lett.* **80**, 1130 (1998).
6. E. Timmermans, *Phys. Rev. Lett.* **81**, 5718 (1998).
7. P. Ao, S. T. Chui, *Phys. Rev. A* **58**, 4836 (1998).
8. M. Zaccanti, C. D'Errico, F. Ferlaino, G. Roati, M. Inguscio, G. Modugno, *Phys. Rev. A* **74**, 041605(R) (2006).
9. S. Ospelkaus, C. Ospelkaus, L. Humbert, K. Sengstock, K. Bongs, *Phys. Rev. Lett.* **97**, 120403 (2006).
10. A. Simoni, F. Ferlaino, G. Roati, G. Modugno, M. Inguscio, *Phys. Rev. Lett.* **90**, 163202 (2003).
11. S. Inouye, J. Goldwin, M. L. Olsen, C. Ticknor, J. L. Bohn, D. S. Jin, *Phys. Rev. Lett.* **93**, 183201 (2004).
12. F. Ferlaino, C. D'Errico, G. Roati, M. Zaccanti, M. Inguscio, G. Modugno, A. Simoni, *Phys. Rev. A* **73**, 040702(R) (2006).
13. C. A. Stan, M. W. Zwierlein, C. H. Schunck, S. M. F. Raupach, W. Ketterle, *Phys. Rev. Lett.* **93**, 143001 (2004).
14. I. Ferrier-Barbut, M. Delehaye, S. Laurent, A. T. Grier, M. Pierce, B. S. Rem, F. Chevy, C. Salomon, *Science* **345**, 1035 (2014).
15. V. D. Vaidya, J. Tiamsuphat, S. L. Rolston, J. V. Porto, *Phys. Rev. A* **92**, 043604 (2015).
16. X.-C. Yao, H.-Z. Chen, Y.-P. Wu, X.-P. Liu, X.-Q. Wang, X. Jiang, Y. Deng, Y.-A. Chen, J.-W. Pan, *Phys. Rev. Lett.* **117**, 145301 (2016).
17. R. Roy, A. Green, R. Bowler, S. Gupta, *Phys. Rev. Lett.* **118**, 055301 (2017).
18. B. J. DeSalvo, K. Patel, J. Johansen, C. Chin, *Phys. Rev. Lett.* **119**, 233401 (2017).
19. B. J. DeSalvo, K. Patel, G. Cai, C. Chin, *Nature* **568**, 61 (2019).
20. S.-K. Tung, C. Parker, J. Johansen, C. Chin, Y. Wang, P. S. Julienne, *Phys. Rev. A* **87**, 010702(R) (2013).

21. S. K. Tung, K. Jimenez-Garcia, J. Johansen, C. V. Parker, C. Chin, *Phys. Rev. Lett.* **113**, 240402 (2014).
22. J. Johansen, B. J. DeSalvo, K. Patel, C. Chin, *Nature Phys.* **13**, 731 (2017).
23. J. Ulmanis, S. Häfner, R. Pires, E. D. Kuhnle, M. Weidemüller, E. Tiemann, *New J. Phys.* **17**, 055009 (2015).
24. M. Repp, R. Pires, J. Ulmanis, R. Heck, E. D. Kuhnle, M. Weidemüller, E. Tiemann, *Phys. Rev. A* **87**, 010701(R) (2013).
25. T. Karpiuk, K. Brewczyk, S. Ospelkaus-Schwarzer, K. Bongs, M. Gajda, K. Rzazewski, *Phys. Rev. Lett.* **93**, 100401 (2004).
26. S. K. Adhikari, *Phys. Rev. A* **72**, 053608 (2005).
27. F. Dalfovo, S. Giorgini, L. P. Pitaevskii, S. Stringari, *Rev. Mod. Phys.* **71**, 463 (1999).
28. E.P. Gross, *Nuovo Cimento* **20**, 454 (1961).
29. L.P. Pitaevskii, *Sov. Phys. JETP* **13**, 451 (1961).
30. S. Giorgini, L. P. Pitaevskii, S. Stringari, *Rev. Mod. Phys.* **80**, 1215 (2008).
31. T. K. Ghosh, K. Machida, *Phys. Rev. A* **73**, 025601 (2006).
32. Y. E. Kim, A. L. Zubarev, *Phys. Rev. A* **72**, 011603(R), (2005).
33. N. Manini, L. Salasnich, *Phys. Rev. A*, **71**, 033625 (2005).
34. Y. Chen, K.-Z. Zhang, Y.-L. He, Z.-L. Liu, L. Zhu, *Int J Theor Phys* **57** 250 (2018).
35. W. Wen, C. Zhao, X. Ma, *Phys. Rev. A* **88**, 063621 (2013).
36. S. Gautam, P. Muruganandam, D. Angom, *Phys. Rev. A* **83**, 023605 (2011).
37. J. Yin, Y.-I. Ma, G. Huang, *Phys. Rev. A* **74**, 013609 (2006).
38. S. K. Adhikari, L. Salasnich, *Phys. Rev. A* **77**, 033618 (2008).
39. S. K. Adhikari, L. Salasnich, *Phys. Rev. A* **78**, 043616 (2008).
40. S. K. Adhikari, *Phys. Rev. A* **77**, 045602 (2008).
41. S. Gautam, S.K. Adhikari, *Phys. Rev. A* **100**, 023626 (2019).
42. J. Li, W. Wen, Y. Wang, X. Ma, H. Li, *Phys. Lett. A* **410**, 127543 (2021).
43. W. Wen, H.-j. Li, *New J. Phys.* **20**, 083044 (2018).
44. P. Díaz, D. Laroze, A. Ávila, B. A. Malomed, *Commun. Nonlin. Sci. Num. Simul.* **70**, 372 (2019).
45. H. Sakaguchi, B. A. Malomed, *Phys. Rev. Research* **2**, 033188 (2020).
46. W. Wen, T. Shui, Y. Shan, C. Zhu, *J. Phys. B* **48**, 175301 (2015).
47. T. D. Lee, C.N. Yang, *Phys. Rev.* **105**, 1119 (1957).
48. T. D. Lee, K. Huang, C.N. Yang, *Phys. Rev.* **106**, 1135 (1957).
49. K. Huang, C. N. Yang, *Phys. Rev.* **105**, 767 (1957).
50. L. Salasnich, A. Parola, L. Reatto, *Phys. Rev. A* **72**, 025602 (2005).
51. A. Bulgac, G. F. Bertsch, *Phys. Rev. Lett.* **94**, 070401 (2005).
52. F. M. Marchetti, Th. Jolicoeur, M. M. Parish, *Phys. Rev. Lett.* **103**, 105304 (2009).
53. S. K. Adhikari, B. A. Malomed, L. Salasnich, F. Toigo, *Phys. Rev. A* **81**, 053630 (2010).
54. P. Siegl, S. I. Mistakidis, P. Schmelcher, *Phys. Rev. A* **97**, 053626 (2018).
55. R. Liao, *Phys. Rev. Research* **2**, 043218 (2020).
56. J. Nisperuza, J. P. Rubio, R. Avella, *J. Phys. Commun* **6**, 025004 (2022).
57. S. K. Adhikari, L. Salasnich, *Phys. Rev. A* **76**, 023612 (2007).
58. G. E. Astrakharchik, J. Boronat, J. Casulleras, S. Giorgini, *Phys. Rev. Lett.* **93**, 200404 (2004).
59. G. E. Astrakharchik, R. Combescot, X. Leyronas, S. Stringari, *Phys. Rev. Lett.* **95**, 030404 (2005).
60. U. Eismann, L. Khaykovich, S. Laurent, I. Ferrier-Barbut, B. S. Rem, A. T. Grier, M. Delehay, F. Chevy, C. Salomon, L.-C. Ha, C. Chin, *Phys. Rev. X* **6**, 021025 (2016).
61. W. Li, T.-L. Ho, *Phys. Rev. Lett.* **108**, 195301 (2012).

-
62. P. Makotyn, C. E. Klauss, D. L. Goldberger, E. A. Cornell, D. S. Jin, *Nature Phys.* **10**, 116 (2014).
 63. C. Eigen, J. A. P. Glidden, R. Lopes, N. Navon, Z. Hadzibabic, R. P. Smith, *Phys. Rev. Lett.* **119**, 250404 (2017).
 64. J. Bardeen, L. N. Cooper, J. R. Schrieffer, *Phys. Rev.* **106**, 162 (1957).
 65. C. F. von Weizsäcker, *Zeits. für Physik* **96**, 431 (1935).
 66. P. Capuzzi, A. Minguzzi, M. P. Tosi, *Phys. Rev. A* **68**, 033605 (2003).
 67. M. Centelles, M. Guilleumas, M. Barranco, R. Mayol, M. Pi, *Laser Phys.* **16**, 360 (2006).
 68. D. M. Jezek, M. Barranco, M. Guilleumas, R. Mayol, M. Pi, *Phys. Rev. A* **70**, 043630 (2004).
 69. M. Guilleumas, M. Centelles, M. Barranco, R. Mayol, M. Pi, *Phys. Rev. A* **72**, 053602 (2005).
 70. S. K. Adhikari, L. Salasnich, *New J. Phys.* **11**, 023011 (2009).
 71. P. Muruganandam, S. K. Adhikari, *Comput. Phys. Commun.* **180**, 1888 (2009).
 72. D. Vudragović, I. Vidanović, A. Balaž, P. Muruganandam, S. K. Adhikari, *Comput. Phys. Commun.* **183**, 2021 (2012).
 73. L. E. Young-S., P. Muruganandam, S. K. Adhikari, V. Loncar, D. Vudragović, A. Balaž, *Comput. Phys. Commun.* **220**, 503 (2017).
 74. S. Röthel, A. Pelster, *Eur. Phys. J. B* **59**, 343 (2007).
 75. Y. Ding and C. H. Greene, *Phys. Rev. A* **95**, 053602 (2017).
 76. S. Y. Chang, V. R. Pandharipande, J. Carlson, and K. E. Schmidt, *Phys. Rev. A* **70**, 043602 (2004).
 77. S. Pilati and S. Giorgini, *Phys. Rev. Lett.* **100**, 030401 (2008).
 78. N. Navon, S. Nascimbène, F. Chevy, and C. Salomon, *Science* **328**, 729 (2010).
 79. M. Horikoshi, M. Koashi, H. Tajima, Y. Ohashi, and M. Kuwata-Gonokami, *Phys. Rev. X* **7**, 041004 (2017).
 80. M. J. H. Ku, A. T. Sommer, L. W. Cheuk, and M. W. Zwierlein, *Science* **335**, 563 (2012).